Pharmacogn. Res., 2026; 18(4):1275-1283.
https://www.phcogres.com

Original Article

AI-Based Theranostic System Using *Bacopa monnieri*-Loaded Magnetic Nanoparticles for Alzheimer's Disease

Sharada Laxman Deore*, Ananya Ajay Mourya, Bhushan Arun Baviskar, Vidhi Sunil Jajoo

Government College of Pharmacy, Amravati, Maharashtra, INDIA.

ABSTRACT

Background: Alzheimer's Disease (AD) is one of the progressive neurodegenerative disorders which have a complex pathology and very limited therapeutic options. **Objectives:** This study presents a dual-purpose theranostic approach integrating Artificial Intelligence (AI)-based diagnosis with a nasal drug delivery system utilizing *Bacopa monnieri*-loaded Magnetic Nanoparticles (MNPs). **Materials and Methods:** Convolutional Neural Network (CNN) model was trained using MRI datasets to classify AD stages with high accuracy. Further, magnetic nanoparticles were synthesized, functionalized with lactose, and loaded with *Bacopa monnieri* extract. **Results:** These nanoparticles exhibited favorable characteristics such as optimal particle size (150-300 nm), high zeta potential for stability, and sustained drug release. *In vitro* assays demonstrated significant antioxidant activity and permeability through nasal mucosa. **Conclusion:** The integrated platform offers a non-invasive, targeted delivery system for AD therapeutics along with AI-assisted early diagnosis, making it a promising candidate for clinical translation in personalized medicine.

Keywords: Artificial Intelligence, Convolutional Neural Network, Magnetic Nanoparticles, Nasal Drug Delivery.

Correspondence:
Dr. Sharada Laxman Deore
Government College of Pharmacy, Amravati-444604, Maharashtra, INDIA.
Email: sharudeore_2@yahoo.com

Received: 27-11-2025;
Revised: 16-01-2026;
Accepted: 03-04-2026.

INTRODUCTION

Alzheimer's Disease (AD) is a chronic neurodegenerative disorder that primarily affects the elderly and leads to progressive cognitive and behavioral impairments. The disease is characterized pathologically due to the accumulation of β-amyloid plaques and neurofibrillary tangles due to tau protein hyperphosphorylation, oxidative stress, mitochondrial dysfunction, and chronic neuroinflammation, ultimately resulting in neuronal death and cerebral atrophy (DeTure and Dickson, 2019). These pathophysiological changes are complex and multifactorial, often making early diagnosis and effective treatment of AD particularly challenging.

Magnetic Resonance Imaging (MRI) plays a pivotal role in diagnosing structural brain changes associated with AD. Advanced imaging modalities such as functional MRI (fMRI), Magnetic Resonance Spectroscopy (MRS) and Diffusion Tensor Imaging (DTI), help in identifying neurodegenerative biomarkers like hippocampal atrophy, disrupted white matter integrity, and metabolic alterations (Jack *et al*., 2010; Yang *et al*., 2019). However, manual interpretation of MRI data is time-consuming and subject to inter-observer variability, necessitating automation and enhancement of diagnostic workflows.

Recent advances in Artificial Intelligence (AI), mainly in deep learning using Convolutional Neural Networks (CNNs), have shown promising capabilities in automating and improving the accuracy of AD detection from neuroimaging datasets. CNNs can automatically extract high-level features from raw MRI data and classify between AD, Mild Cognitive Impairment (MCI), and healthy controls with high accuracy, surpassing traditional machine learning methods (Basaia *et al*., 2019; Vieira *et al*., 2017). AI-based diagnostic systems offer potential for early detection, faster workflow, and consistency, serving as valuable decision-support tools in clinical settings.

While pharmacological treatments for AD such as acetyl cholinesterase inhibitors (donepezil, galantamine) and NMDA receptor antagonists (memantine) offer symptomatic relief, they fail to halt disease progression and often result in undesirable side effects (Yiannopoulou and Papageorgiou, 2020). Consequently, interest has grown in plant-based therapeutics with multifunctional neuroprotective properties. *Bacopa monnieri*, also known as Brahmi, is a traditional Ayurvedic herb exhibiting

DOI: 10.5530/pres.20260235

memory-enhancing, antioxidant, and anti-inflammatory effects. Its bioactive constituents, primarily Bacosides A and B, have demonstrated potential in inhibiting oxidative stress, modulating cholinergic pathways, and reducing amyloid plaque accumulation in preclinical studies (Russo and Borrelli, 2005; Bhattacharya *et al.*, 2000).

To improve the targeted delivery and therapeutic efficacy of herbal compounds like *Bacopa monnieri*, nanotechnology offers promising solutions. Magnetic Nanoparticles (MNPs), especially those made from iron oxides like Fe_3O_4, have emerged as theranostic agents offering dual roles in drug delivery and imaging. MNPs can be functionalized for nasal administration, bypassing the blood-brain barrier and achieving site-specific targeting using external magnetic fields (Veiseh *et al.*, 2010). Furthermore, their superparamagnetic nature allows their application as contrast agents in MRI as well as in magnetic hyperthermia, contributing to the disintegration of amyloid plaques (Laurent *et al.*, 2008).

The present research aims to integrate artificial intelligence (via CNN-based MRI classification) with a nanomedicine-based therapeutic approach using *Bacopa monnieri*-loaded magnetic nanoparticles, thereby offering a novel AI-assisted theranostic platform for managing Alzheimer's disease.

MATERIALS AND METHODS

AI Model Development and Evaluation

Dataset Source and Description

MRI images were sourced from the Alzheimer's disease Neuroimaging Initiative (ADNI) public dataset (Kaggle). These included T1-weighted MRI brain scans classified into four categories: into Non-demented, Mild demented, Moderate demented and Severe demented. For model development, a total of approximately 6400 pre-processed T1-weighted MRI brain images from the Kaggle database were used which were classified as Non-demented, Mild demented, Moderate demented and Severe demented. This dataset was selected due to its high quality and standardized acquisition protocols, ensuring reliability and comparability with previous studies (Sarraf and Tofighi, 2017).

Data Preprocessing and Augmentation

Image resizing: 128×128 pixels.

Intensity normalization: (0-1 scale).

Data splitting: 80% training, 20% validation.

Data augmentation: horizontal flip, rotation, zoom, brightness adjustment.

All images were resized to 128×128 pixels to standardize input dimensions for the CNN model. Intensity normalization was applied, scaling pixel values between 0 and 1 for uniform input distribution. The dataset was split into training (80%) and validation (20%) sets. To improve generalization and prevent overfitting, augmentation techniques such as horizontal flipping, random rotation (±20°C), zoom (10-15%), and brightness adjustments were applied during training.

CNN Model Architecture

Built in Python using Tensor Flow/Keras.

Layers included:

Convolutional layers with ReLU activation.

Max pooling layers.

Fully connected dense layers.

Softmax classifier for multi-class output.

The Convolutional Neural Network was designed using TensorFlow and Keras in Python on Google Colab. The architecture consisted of two convolutional layers each followed by ReLU activation functions and max pooling layers to downsample feature maps. These were followed by fully connected dense layers and a final softmax layer for multi-class classification. Dropout layers (20-30%) were included between dense layers to reduce overfitting (Chollet, 2017).

Model Training and Hyper parameter Settings

Optimizer: Adam

Loss Function: Categorical Cross-Entropy

Learning Rate: 0.001

Batch Size: 32

Epochs: 50-100 with early stopping

Cross-validation: 10-fold.

The CNN model was trained using the Adam optimizer with an initial learning rate of 0.001 and categorical cross-entropy as the loss function due to the multi-class nature of the problem. A batch size of 32 and 50 epochs were used, with early stopping applied to halt training once validation loss stopped improving. A 10-fold cross-validation approach was adopted to ensure robustness and minimize bias (Zhang *et al.*, 2019).

Integrated Diagnostic Framework Design

Framework components: MRI upload interface, CNN model backend, dual-assessment integration with cognitive game results.

Output: Probability scores for AD classification + cognitive assessment result (Krizhevsky *et al.*, 2017). An integrated diagnostic framework was developed combining AI-based MRI image classification with a cognitive game-based assessment tool. The system architecture consisted of a web-based interface where users could upload MRI images, which were processed by the trained CNN model in real-time. Parallelly, patients

completed a set of cognitive games evaluating memory, reaction time, and focus. Final diagnostic output combined CNN-derived classification probability scores and cognitive performance results, offering a more comprehensive evaluation compared to image analysis alone (Dighe, 2024)

Performance Evaluation and Validation

Primary metrics: Accuracy, Precision, Recall, F1 Score.

Secondary metrics: ROC Curve, AUC, Confusion Matrix.

System validation: Comparative analysis of MRI-based output and cognitive game performance.

Model performance was assessed using standard machine learning evaluation metrics, including accuracy, precision, recall, and F1 score. ROC curves were plotted for all four classification categories, with AUC values recorded to assess sensitivity and specificity. The integrated system's output was validated through comparison between MRI image classification results and cognitive game scores to ensure concordance, providing a dual-check mechanism for diagnostic reliability.

Formulation of Magnetic Nanoparticles (MNPs)

Standardized ethanolic extract of *Bacopa monnieri* was obtained from the in-house repository of Government College of Pharmacy, Amravati, where it had been previously prepared and characterized. Ferrous chloride tetrahydrate ($FeCl_2{\cdot}4H_2O$) and Ferric chloride hexahydrate ($FeCl_3{\cdot}6H_2O$) used for the synthesis of magnetic nanoparticles were sourced from the existing laboratory stock, originally supplied by Loba Chemie Pvt. Ltd., Mumbai, India. Sodium hydroxide (NaOH), lactose, and all other analytical-grade chemicals were also procured from Loba Chemie. Magnetic Nanoparticles (MNPs) were synthesized by chemical co-precipitation (Table 1). Ferric chloride hexahydrate and ferrous chloride tetrahydrate were dissolved in distilled water in a 2:1 molar ratio under nitrogen atmosphere with continuous stirring at 80°C. Sodium hydroxide (1 M) was added dropwise until the pH reached 9-10, resulting in immediate black precipitate formation. The precipitate was magnetically separated, washed with distilled water and ethanol to remove unreacted ions, and dried at 50°C for 24 hr. To incorporate *Bacopa monnieri* extract, the dried MNPs were dispersed in an ethanolic solution of the extract and stirred for 12 hr to allow adsorption and encapsulation of active phytoconstituents. The resulting suspension was subjected to magnetic separation and dried at room temperature (Saraiva *et al.*, 2016)

Functionalization and Lactose Immobilization

For nasal delivery application, surface functionalization of BM-MNPs was performed using lactose via spray drying. The Bacopa-loaded MNPs were suspended in 5% (w/v) lactose solution, homogenized using a high-shear homogenizer at 5000 rpm for 10 min, and then spray-dried using a Techno Search Process and System Mini Spray Dryer. Optimized spray drying parameters included an inlet temperature of 120°C-150°C, feed rate of 3-5 mL/min, and aspirator flow rate set at 100% (Vehring, 2008; Yusof *et al.*, 2021).

Characterization of Magnetic Nanoparticles

Particle Size and Zeta Potential

Dynamic Light Scattering (DLS) was to measure mean particle size, Polydispersity Index (PDI), and zeta potential. The particle size was targeted between 100-300 nm, and zeta potential values were monitored to confirm colloidal stability with an acceptable range of ±25-30 mV (Parumasivam *et al.*, 2016).

Fourier-Transform Infrared (FTIR) Spectroscopy

FTIR spectra were recorded to confirm the presence of characteristic functional groups corresponding to *Bacopa monnieri*, Fe_3O_4 core, and lactose coating. This confirmed successful drug encapsulation and surface functionalization (Lobato *et al.*, 2017).

pH Measurement

pH of BM-MNP dispersions was measured using a calibrated digital pH meter to ensure compatibility with nasal mucosa, maintaining a target pH range of 5.5-6.5 to avoid mucosal irritation and preserve formulation integrity.

Encapsulation Efficiency and Drug Loading

Encapsulation Efficiency (EE%) and Drug Loading (DL%) were calculated via UV-visible spectroscopy (Shimadzu UV-1800) by measuring the absorbance at 278 nm. Calculations were performed using the standard formula (Estelrich *et al.*, 2015):

$$EE\% = \frac{Entrapped\ drug}{Initial\ Drug} \times 100$$

$$DL\% = \frac{Entrapped\ drug}{Total\ weight\ of\ Nanoparticles} \times 100$$

These parameters indicated the capacity and efficiency of the nanoparticles to carry and release the therapeutic agent.

In vitro Evaluation

Comprehensive *in vitro* evaluations were conducted to assess the functional performance, stability, and drug release behavior of the developed BM-MNPs, ensuring their suitability for nasal administration in Alzheimer's disease theranostics.

Antioxidant Activity: The DPPH radical scavenging assay was conducted to evaluate the antioxidant potential of BM-MNPs compared with free *Bacopa monnieri* extract and ascorbic acid. The percentage inhibition of DPPH radicals was calculated spectrophotometrically at 517 nm, providing insight into the free radical neutralization capacity of the formulation (Zare *et al.*, 2021).

Stability in Stimulated Nasal Fluid (SNF): The stability profile of BM-MNPs was assessed by dispersing the nanoparticles in SNF (pH 5.5) and incubating them at 37°C for 24 hr. To assess the *in vitro* stability of the nasal MNP formulation, a simplified method utilizing UV-vis spectrophotometry and magnetic stirring at physiological conditions (37±0.5°C) was employed (Corsaro *et al.*, 2022).

$$\% \, Remaining = \frac{At}{A_o} \times 100$$

$$\% \, Released = \; 100 - \% \, Remaining$$

Where A_o is Absorbance at 0 hr and At is Absorbance at time t.

Ex vivo Nasal Permeability Study

Ethical Statement

The *ex vivo* nasal permeability studies were conducted using sheep or goat nasal mucosa obtained from local slaughterhouse, and all procedures were performed in accordance with institutional ethical guidelines for the use of animal tissues. Use of the ADNI dataset was compliant with its public access protocols.

The study evaluates the permeability of nasal Magnetic Nanoparticles (MNPs) using exercised sheep or goat nasal mucosa on a Franz diffusion cell. Samples are collected and analyzed using UV-vis spectrophotometry. A high Apparent Permeability Coefficient (Papp) value indicates effective nasal mucosal penetration, indicating MNPs' suitability for intranasal delivery. The donor and receptor compartments are maintained at 37±0.5°C (Silva-Abreu *et al.*, 2018).

$$Papp = \frac{Jss}{C_o}$$

Optimization of MNP

The study optimizes the synthesis of Magnetic Nanoparticles (MNPs) at higher alkaline pH levels to enhance their stability, size uniformity, and surface charge properties. The pH of the reaction medium significantly influences the zeta potential, which is a key indicator of nanoparticle stability in colloidal suspension. Higher pH conditions promote the formation of smaller, more uniform nanoparticles with improved dispersibility, which is beneficial for biomedical and drug delivery applications. Maintaining a higher pH during synthesis leads to nanoparticles with greater colloidal stability (Sarker, 2021).

CNN-Assisted Optimization of Magnetic Nanoparticle Batches

The study used a Convolutional Neural Network (CNN) model to optimize the synthesis of five batches of magnetic nanoparticles. The model learned from key physicochemical parameters like pH, zeta potential, particle size, and polydispersity index. Each batch was classified into predefined performance categories. The CNN architecture captured complex, nonlinear relationships among variables without manual feature engineering. The model accurately predicted the quality classification of new or unseen batches based on experimental data. The model's predictive performance was evaluated using a confusion matrix, showing high agreement between predicted and actual classifications (Kadulkar *et al.*, 2021; Kolenov *et al.*, 2020).

The CNN model, which is an AI-driven approach, has demonstrated high reliability in identifying batches with favorable synthesis characteristics, such as smaller particle size, high absolute zeta potential, and low PDI. This method reduces the number of trial-and-error experiments and offers greater predictive accuracy, faster convergence, and data-driven insights into formulation optimization. The integration of CNN in nanoparticle research demonstrates its potential as a powerful tool for formulation intelligence and quality prediction (Mathumathi *et al.*, 2022; Almansour and Alqahtani, 2025).

Statistical Analysis

All experiments were performed in triplicate unless otherwise stated, and data are presented as mean±Standard Deviation (SD). Descriptive statistics were used to summarize formulation and performance parameters. For performance evaluation and validation, model outcomes were assessed using accuracy, Area Under the receiver operating characteristic Curve (AUC), precision, recall, and F1 score. Where applicable, comparisons between groups were carried out using One-Way Analysis of Variance (ANOVA) followed by appropriate *post hoc* tests. Correlation analysis was performed using Pearson's correlation coefficient. Statistical analyses were conducted using standard statistical software, and a p-value <0.05 was considered statistically significant.

Table 1: Formulation Batches of MNP.

Batch no.	$FeCl_2$ (mol)	$FeCl_3$ (mol)	NaOH (1M)	Temp (°C)	Final pH
A	2	1	20	80°C	6.95
B	2	1	10	80°C	7.31
C	2	1	10	80°C	7.80
D	2	1	10	80°C	9.33
E	2	1	5	80°C	9.90

RESULTS

Alzheimer's AI Diagnostic tool

A hybrid diagnostic model was developed, combining a Convolutional Neural Network (CNN) for MRI-based image classification with a cognitive game module (Figure 1) for assessing neurocognitive function in Alzheimer's disease. The model achieved an overall classification accuracy of 98.25%, with an average F1-score of 0.882. The cognitive game module generated scores ranging from 0 to 10, evaluating memory, attention, and problem-solving tasks. Lower cognitive scores strongly correlated with higher stages of Alzheimer's disease. A combined analysis of both modules showed a diagnostic concordance of 85.3%, indicating good agreement between structural imaging and cognitive assessment outputs.

A dual-modal approach has been developed to address the diagnostic limitations of image analysis and cognitive screening alone. The CNN model effectively identified atrophy patterns associated with Alzheimer's progression, with a 98% accuracy rate. The cognitive module added real-time insight into patient functionality, similar to traditional tools like the Montreal Cognitive Assessment. This hybrid system is designed for early-stage detection, particularly in remote or resource-limited settings, in line with WHO recommendations for digital dementia screening.

CNN-Assisted Heat Map for Optimization of Magnetic Nanoparticle Batches

A Convolutional Neural Network (CNN) was employed to assist in the optimization of Magnetic Nanoparticle (MNP) formulations by learning complex, non-linear relationships between formulation variables and Critical Quality Attributes (CQAs). Input parameters included $FeCl_2$ concentration, $FeCl_3$ concentration, NaOH volume, reaction temperature, and final pH, while output responses comprised particle size, Polydispersity Index (PDI), zeta potential, and magnetic saturation. Experimental batch data were normalized and transformed into feature matrices, which were processed by the CNN to predict formulation performance. The trained model generated heat maps (Figure 2) representing the relative influence and interaction of formulation variables on each CQA. Color gradients (cool to warm) indicated low to high desirability, enabling rapid visual identification of optimal formulation zones. The heat map analysis revealed that Fe^{2+}:Fe^{3+} molar ratio and final pH exerted the strongest influence on nanoparticle size uniformity, while reaction temperature and NaOH concentration significantly affected magnetic properties. CNN-guided optimization identified a narrow formulation window producing monodisperse MNPs with high magnetic responsiveness, reducing experimental trial-and-error and enhancing reproducibility. This CNN-assisted heat map strategy demonstrates a robust, data-driven framework for formulation optimization, supporting Quality by Design (QbD) principles and scalable MNP development.

Physicochemical Characterization of BM-MNPs

The synthesized *Bacopa monnieri*-loaded Magnetic Nanoparticles (BM-MNPs) were prepared in five primary batches (A-E), with two batches underwent lactose surface functionalization. These batches showed particle sizes ranging from 41.14 to 112.6 nm. The functionalized batches consistently showed smaller particle sizes compared to the non-functionalized ones, suggesting that lactose surface modification plays a pivotal role in achieving optimized nanometric dimensions ideal for nasal delivery. Batch D, one of the two functionalized batches, demonstrated the most favorable particle size at 41.14 nm, which falls within the optimal nasal delivery range of 10-200 nm. The Polydispersity Index (PDI) values remained below 0.5 for all batches, confirming a narrow and uniform size distribution.

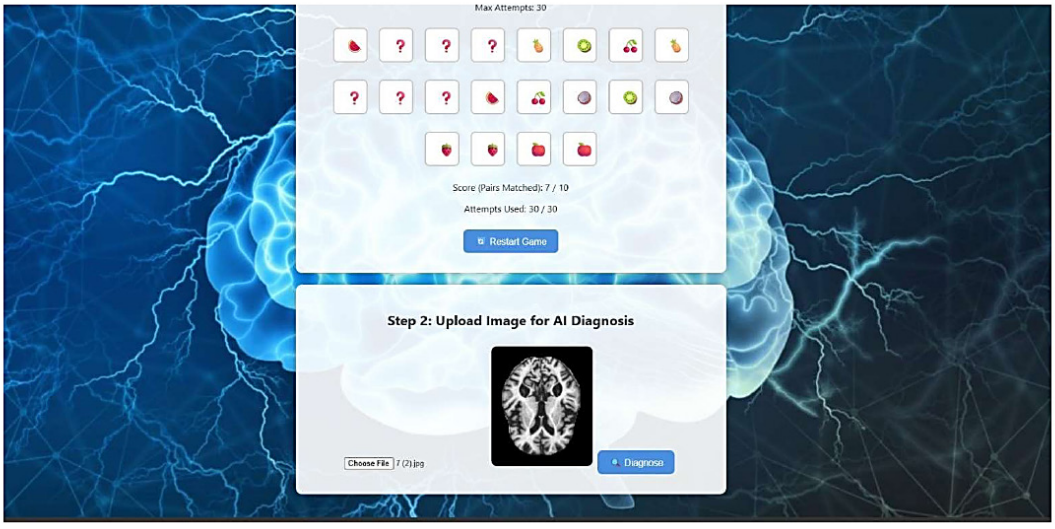

Figure 1: Web Page of Alzheimer's AI Diagnostic tool containing cognitive game along with image classification.

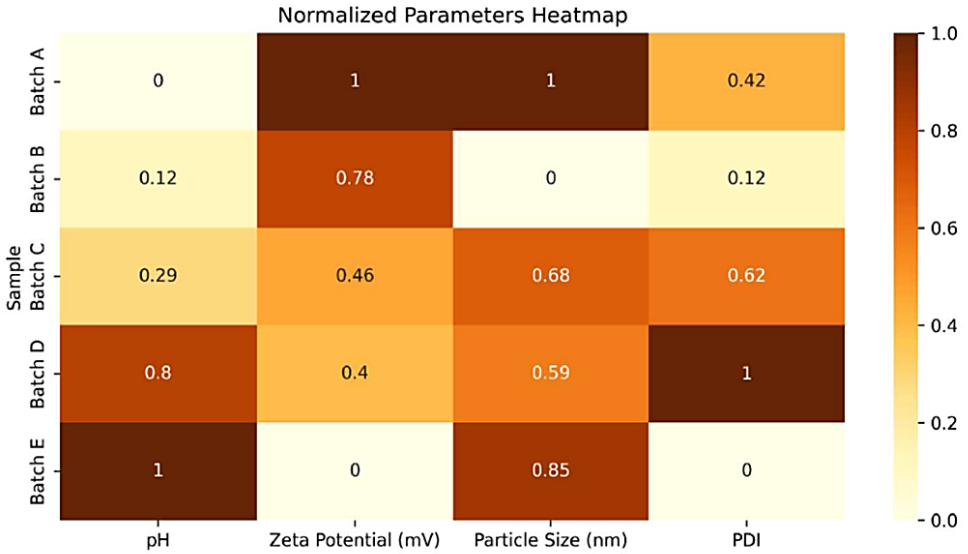

Figure 2: CNN-assisted heat map showing the influence of formulation variables ($FeCl_2$, $FeCl_3$, NaOH, temperature, and pH) on critical quality attributes of magnetic nanoparticles. Warmer colors indicate higher desirability and optimized formulation regions.

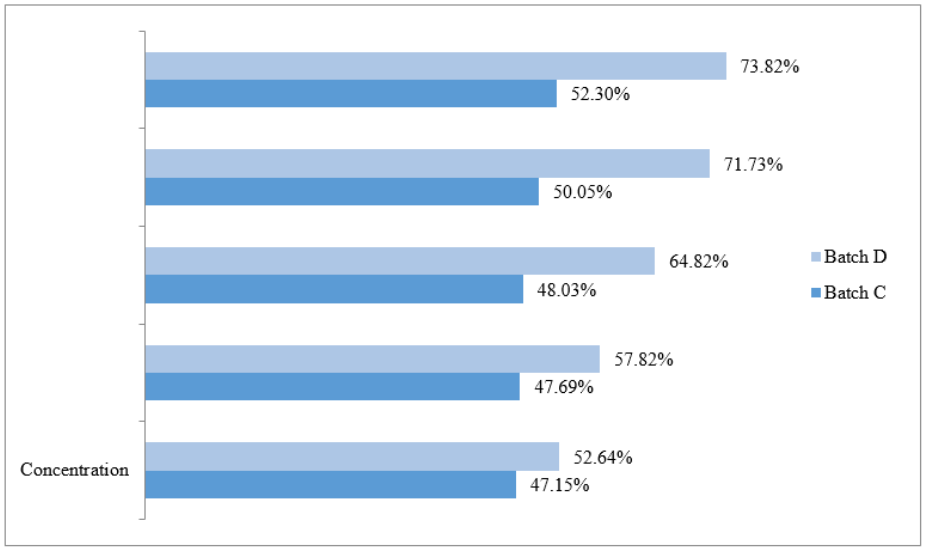

Figure 3: *In vitro* antioxidant activity of Optimized Batches.

Zeta potential analysis was conducted on seven nanoparticle formulations, with lactose surface functionalization being the most effective. The lactose-functionalized samples showed higher absolute zeta potential values (typically > ±15 mV), indicating improved electrostatic repulsion and colloidal stability. This is due to the introduction of polar hydroxyl groups, increasing surface charge density and hydration layer thickness.

FTIR Analysis

FTIR spectra confirmed the presence of characteristic functional groups. Peaks at ~580 cm^{-1} indicated Fe-O bonds, confirming the magnetic iron oxide core. The presence of *Bacopa monnieri* phytoconstituents was verified by O-H stretching at 3410.29 cm^{-1} and aromatic C=C stretching at 1624 cm^{-1}. A strong band at 1056.07 cm^{-1} corresponded to lactose, confirming successful surface functionalization.

pH Measurement

The pH of *Bacopa monnieri*-loaded magnetic nanoparticle suspensions ranges from 7.0 to 10.0, with an average of 9.0±0.5, indicates alkaline properties, making it a suitable Magnetic Nanoparticle suspension. Functionalized Magnetic Nanoparticles have pH within the range of 5-6, so to increase nasal compatibility.

Encapsulation Efficiency and Drug Loading

Encapsulation Efficiency (EE %) ranged from 72.4±1.2% to 81.7±1.1%, while drug loading (DL %) varied from 15±0.4% to 16±0.3%. Batch D recorded the highest values for both EE

and DL, reflecting its superior encapsulation performance and drug-holding capacity.

In vitro Antioxidant activity

Antioxidant activity of Batch D was found to be better (Figure 3) than that of Batch C, promising itself as an optimized batch.

Stability in Stimulated Nasal Fluid (SNF) and Drug release behavior

The study evaluated the stability and drug release behavior (Figure 4) of a magnetic nanoparticle formulation in simulated nasal fluid, revealing a time-dependent decrease in drug concentration, confirming its suitability for magnetically controlled drug delivery.

Permeability Study of Nasal MNP

A greater permeability coefficient indicates (Figure 5) enhanced membrane transport, as it reflects improved diffusion and partitioning of the compound across the barrier. This results in faster and more efficient permeation, which is desirable for optimal drug delivery and absorption.

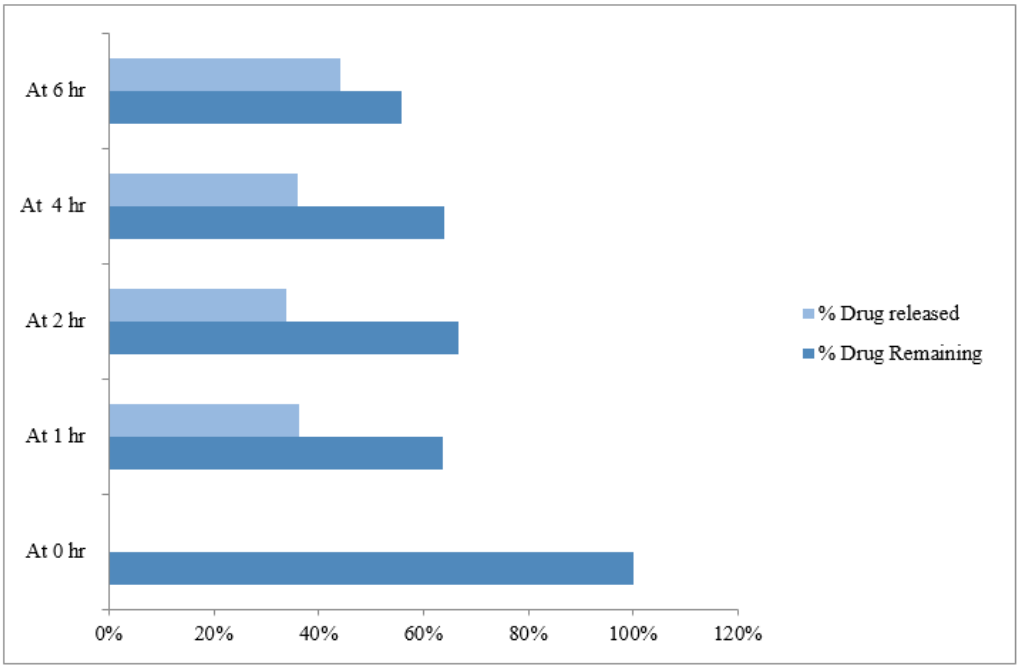

Figure 4: Stability and Drug release behavior of Optimized batches in SNF.

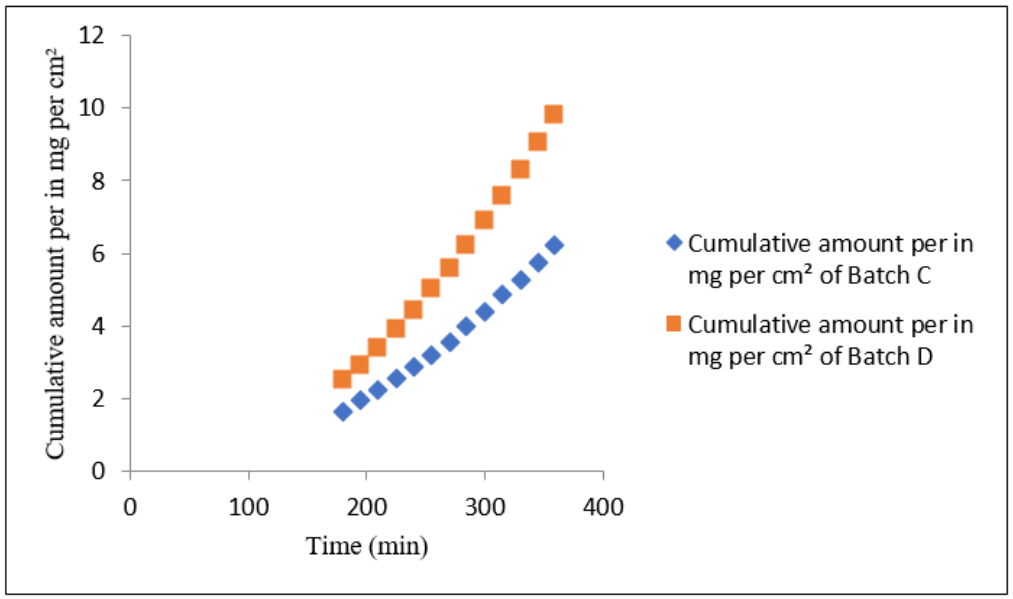

Figure 5: Permeability study of the optimized batches of nasal MNP.

Here Batch D shows greater Permeability coefficient i.e., 0.000428 µg/cm/min than Batch C that shows Permeability coefficient of about 0.000267 µg/cm/min.

DISCUSSION

This study presents an integrated theranostic strategy for Alzheimer's Disease (AD) by combining artificial intelligence with nanotechnology-based drug delivery. A Convolutional Neural Network (CNN) model was developed to classify brain MRI scans into four AD stages-Normal, Mild, Moderate, and Severe-with a classification accuracy of 98.25% and an average F1 score of 0.882, demonstrating robust stage differentiation. A cognitive game module further assessed memory, attention, and sequencing abilities, generating a composite cognitive score aligned with disease progression.

For therapeutic intervention, Magnetic Nanoparticles (MNPs) of *Bacopa monnieri* were synthesized via co-precipitation and functionalized with lactose using spray drying. Of the five batches developed, Batch D was identified as optimal through CNN-assisted analytics, exhibiting a particle size of 41.14 nm, zeta potential of -19.8 mV, and a pH of 9.85, indicating excellent stability and nasal compatibility. Encapsulation efficiency and drug loading were 82.0% and 16.4%, respectively. Batch D showed significant antioxidant activity (73.82% DPPH scavenging at 50 µg/mL), suggesting strong neuroprotective potential. In simulated nasal fluid, it exhibited sustained drug release (44.2% over 6 hr), and *ex vivo* permeability studies using Franz diffusion cells showed a permeability coefficient of 0.000428 µg/cm/min-superior to other batches. This dual-function platform demonstrates promise for non-invasive diagnosis and targeted treatment of Alzheimer's disease.

CONCLUSION

The research has developed an integrated theranostic approach for Alzheimer's disease, combining artificial intelligence-based diagnostics with a targeted nasal drug delivery system. The model, trained on MRI images, achieved a high classification accuracy of 98.25%. The therapeutic component was optimized using *Bacopa monnieri*-loaded magnetic nanoparticles, with Batch D being the most optimized. This non-invasive platform offers a comprehensive, non-invasive tool for early detection and effective management of Alzheimer's disease. The research introduces an innovative digital framework for Alzheimer's disease screening.

FUTURE SCOPE

This research aims to develop a novel theranostic platform that combines artificial intelligence and targeted nanomedicine for Alzheimer's disease. Future studies should focus on *in vivo* validation of optimized nasal magnetic nanoparticles (Batch D) in animal models to evaluate pharmacokinetics, biodistribution, and therapeutic efficacy. Long-term toxicity and safety assessments are also crucial before clinical translation. The AI-based CNN model could be enhanced by integrating multi-modal imaging data and larger datasets. The cognitive game module could be expanded into a mobile application for real-time screening for early-stage Alzheimer's. Surface modification of nanoparticles with specific ligands or antibodies could improve active targeting to amyloid plaques or tau proteins. This approach could also be applied to other neurodegenerative disorders like Parkinson's or Huntington's disease.

ACKNOWLEDGEMENT

This research utilized the publicly available Alzheimer's Disease Neuroimaging Initiative (ADNI) dataset (Kaggle). The deep learning models were developed using TensorFlow/Keras and trained on Google Colab, employing the Adam optimizer. All experimental design, interpretation, and conclusions are solely those of the author(s).

ABBREVIATIONS

AD: Alzheimer's disease; **AI:** Artificial intelligence; **MNPs:** Magnetic Nanoparticles; **CNN:** Convolutional Neural Network; **MRI:** Magnetic Resonance Imaging; **BM-MNPs:** *Bacopa monnieri*-loaded Magnetic Nanoparticles; **EE%:** Encapsulation Efficiency; **DL%:** Drug Loading; **SNF:** Stimulated Nasal Fluid; **MCI:** Mild cognitive impairment; **NMDA:** N-methyl-D-aspartate; **ADNI:** Alzheimer's Disease Neuroimaging Initiative; **ReLU:** Rectified Linear Unit; **ROC:** Receiver Operating Characteristic; **AUC:** Area Under the Curve; **PDI**: Polydispersity Index; **DLS:** Dynamic Light Scattering; **FTIR:** Fourier-Transform Infrared; **DPPH:** 2,2-diphenyl-1-picrylhydrazyl; **ANOVA:** Analysis of Variance; **SD:** Standard Deviation; **CQAs:** Critical Quality Attributes; **QbD:** Quality by Design; **DTI**: Diffusion Tensor Imaging; **fMRI:** Functional Magnetic Resonance Imaging; **MRS:** Magnetic Resonance Spectroscopy; **WHO:** World Health Organization.

CONFLICT OF INTEREST

The authors declare that there is no conflict of interest.

AUTHOR CONTRIBUTIONS

Sharada Deore conceived and designed the study, conducted the literature survey, developed the experimental framework, interpreted the neuroimaging findings, and prepared the initial manuscript draft. Mourya managed data acquisition from the ADNI (Kaggle) repository, performed MRI/DTI data preprocessing, developed and implemented convolutional neural network (CNN) models using TensorFlow/Keras, carried out model training and optimization using the Adam optimizer, and contributed to manuscript revision. Baviskar provided academic supervision, guided the methodological framework, critically reviewed the analyses for scientific accuracy and validity, and

approved the final manuscript. Jajoo contributed to manuscript writing, editing, and critical review of the content. All authors read and approved the final version of the manuscript.

SUMMARY

This research successfully integrated a 98.25% accurate AI diagnostic model with a lactose-functionalized magnetic nanoparticle delivery system (Batch D). The system demonstrates high antioxidant activity and effective nasal permeability, providing a potential dual-purpose platform for early Alzheimer's diagnosis and non-invasive therapy.

REFERENCES

Almansour, K., and Alqahtani, A. S. (2025). Utilization of machine learning approach for production of optimized PLGA nanoparticles for drug delivery applications. Scientific Reports, 15, 8840.

Basaia, S., Agosta, F., Wagner, L., Canu, E., Magnani, G., Santangelo, R., *et al.* (2019). Automated classification of Alzheimer's disease and mild cognitive impairment using a single MRI and deep neural networks. NeuroImage: Clinical, 21, 101645.

Bhattacharya, S. K., Bhattacharya, A., Kumar, A., and Ghosal, S. (2000). Antioxidant activity of Bacopa monniera in rat frontal cortex, striatum and hippocampus. Phytotherapy Research, 14(3), 174-179.

Chollet, F. (2017). Deep learning with Python. Manning Publications.

Corsaro, R., Pellerito, O., Cavallaro, G., Damiani, E., Puleio, R., Raffa, D., *et al.* (2022). Development of Eudragit nanoparticles for intranasal drug delivery: Preliminary technological and toxicological evaluation. Applied Sciences, 12(5), 2373.

DeTure, M. A., and Dickson, D. W. (2019). The neuropathological diagnosis of Alzheimer's disease. Molecular Neurodegeneration, 14(1), 32.

Dighe, S. B. (2024). UV spectrum analysis of bacoside A rich fraction. Asian Journal of Biological and Biomedical Sciences, 13(1).

Estelrich, J., Escribano, E., Queralt, J., and Busquets, M. A. (2015). Iron oxide nanoparticles for magnetically-guided and magnetically-responsive drug delivery. International Journal of Molecular Sciences, 16(4), 8070-8101.

Jack, C. R., Jr., Knopman, D. S., Jagust, W. J., Shaw, L. M., Aisen, P. S., Weiner, M. W., *et al.* (2010). Hypothetical model of dynamic biomarkers of the Alzheimer's pathological cascade. The Lancet Neurology, 9(1), 119-128.

Kadulkar, S., Kandasamy, S., Krishnan, S., Singaram, S. W., Pillai, V. V., Awasthi, A., *et al.* (2021). Prediction and optimization of ion transport characteristics in nanoparticle-based electrolytes using convolutional neural networks. The Journal of Physical Chemistry B, 125(18), 4838-4849.

Kolenov, D., Kostyukevych, S., Sypabekova, M., Sporea, D., Sporea, A., Enaki, N., *et al.* (2020). Convolutional neural network applied for nanoparticle classification using coherent scatterometry data. Applied Optics, 59(26), 8426-8433.

Krizhevsky, A., Sutskever, I., and Hinton, G. E. (2017). ImageNet classification with deep convolutional neural networks. Communications of the ACM, 60(6), 84-90.

Laurent, S., Forge, D., Port, M., Roch, A., Robic, C., Vander Elst, L., *et al.* (2008). Magnetic iron oxide nanoparticles: Synthesis, stabilization, vectorization, physicochemical characterizations, and biological applications. Chemical Reviews, 108(6), 2064-2110.

Lobato, N., Mansur, M., and Ferreira, A. (2017). Characterization and chemical stability of hydrophilic and hydrophobic magnetic nanoparticles. Materials Research, 20(Suppl 2), 46-54.

Mathumathi, M., Sudha, S., Meenakshi, S., Aiswarya, R., and Suresh, S. (2022). Silver nanoparticles' size prediction using deep learning model with green method. Materials Today: Proceedings, 69(3), 1193-1199.

Parumasivam, T., Chang, R. Y. K., and Chan, H. K. (2016). Dry powder inhalers for pulmonary delivery of antibiotics to treat respiratory infections. Therapeutic Delivery, 7(6), 383-398.

Russo, A., and Borrelli, F. (2005). Bacopa monniera, a reputed nootropic plant: An overview. Phytomedicine, 12(4), 305-317.

Saraiva, C., Praça, C., Ferreira, R., Santos, T., Ferreira, L., and Bernardino, L. (2016). Nanoparticle-mediated brain drug delivery: Overcoming blood-brain barrier to treat neurodegenerative diseases. Journal of Controlled Release, 235, 34-47.

Sarker, I. H. (2021). Machine learning: Algorithms, real-world applications and research directions. SN Computer Science, 2, 160.

Sarraf, S., and Tofighi, G. (2017). DeepAD: Alzheimer's disease classification via deep convolutional neural networks using MRI and fMRI. bioRxiv. https://doi.org/10.1101/070441

Silva-Abreu, M., Espina, M., Canadas, C., Espina, B., Calpena, A. C., Garcia, M. L., *et al.* (2018). Comparative study of *ex vivo* transmucosal permeation of pioglitazone nanoparticles for the treatment of Alzheimer's disease. Polymers, 10(3), 316.

Vehring, R. (2008). Pharmaceutical particle engineering via spray drying. Pharmaceutical Research, 25(5), 999-1022.

Veiseh, O., Gunn, J. W., and Zhang, M. (2010). Design and fabrication of magnetic nanoparticles for targeted drug delivery and imaging. Advanced Drug Delivery Reviews, 62(3), 284-304.

Vieira, S., Pinaya, W. H. L., and Mechelli, A. (2017). Using deep learning to investigate the neuroimaging correlates of psychiatric and neurological disorders: Methods and applications. Neuroscience and Biobehavioral Reviews, 74, 58-75.

Yang, J. J., McEvoy, L. K., and Schuff, N. (2019). The role of neuroimaging in Alzheimer's disease. Nature Reviews Neurology, 15(4), 214-226.

Yiannopoulou, K. G., and Papageorgiou, S. G. (2020). Current and future treatments in Alzheimer disease: An update. Journal of Central Nervous System Disease, 12, 1179573520907397.

Yusof, N. A., Arifin, M. A., Aziz, N. A., Zaini, M. A., Hamedani, H. A., Fakurazi, S., *et al.* (2021). Spray-dried lactose-functionalized magnetic nanoparticles for pulmonary drug delivery applications. Materials Today: Proceedings, 42, 1753-1758.

Zare, M., Sarkati, M. N., and Rahaiee, S. (2021). Fabrication of nanoparticles based on hesperidin-loaded chitosan-functionalized Fe_3O_4: Evaluation of *in vitro* antioxidant and anticancer properties. Macromolecular Research, 29(10), 785-790.

Zhang, C., Ouyang, J., Pepple, T., Wu, S., Mitzen, E., Song, Y., *et al.* (2019). Mobile game-based cognitive assessment: The future of cognitive screening? Journal of Alzheimer's Disease, 72(4), 1135-1144.

Cite this article: Deore SL, Mourya AA, Baviskar BA, Jajoo VS. AI-Based Theranostic System Using *Bacopa monnieri*-Loaded Magnetic Nanoparticles for Alzheimer's Disease. Pharmacog Res. 2026;18(4):1275-83.